Mitotic protein kinase CDK1 phosphorylation of mRNA translation regulator 4E-BP1 Ser83 may contribute to cell transformation

Celestino Velásquez[a], Erdong Cheng[a], Masahiro Shuda[a], Paula J. Lee-Oesterreich[a], Lisa Pogge von Strandmann[a], Marina A. Gritsenko[b], Jon M. Jacobs[b], Patrick S. Moore[a,1], and Yuan Chang[a,1]

[a]Cancer Virology Program, University of Pittsburgh Cancer Institute, Pittsburgh, PA 15213; and [b]Biological Sciences Division/Biological Systems Analysis & Mass Spectrometry, Pacific Northwest National Laboratory, Richland, WA 99352

Contributed by Yuan Chang, May 16, 2016 (sent for review March 23, 2016); reviewed by James A. DeCaprio and Nahum Sonenberg

Mammalian target of rapamycin (mTOR)-directed eukaryotic translation initiation factor 4E-binding protein 1 (4E-BP1) phosphorylation promotes cap-dependent translation and tumorigenesis. During mitosis, cyclin-dependent kinase 1 (CDK1) substitutes for mTOR and fully phosphorylates 4E-BP1 at canonical sites (T37, T46, S65, and T70) and the noncanonical S83 site, resulting in a mitosis-specific hyperphosphorylated δ isoform. Colocalization studies with a phospho-S83 specific antibody indicate that 4E-BP1 S83 phosphorylation accumulates at centrosomes during prophase, peaks at metaphase, and decreases through telophase. Although S83 phosphorylation of 4E-BP1 does not affect general cap-dependent translation, expression of an alanine substitution mutant 4E-BP1.S83A partially reverses rodent cell transformation induced by Merkel cell polyomavirus small T antigen viral oncoprotein. In contrast to inhibitory mTOR 4E-BP1 phosphorylation, these findings suggest that mitotic CDK1-directed phosphorylation of δ-4E-BP1 may yield a gain of function, distinct from translation regulation, that may be important in tumorigenesis and mitotic centrosome function.

4E-BP | cyclin-dependent kinase 1 | cap-dependent translation | mitosis | Merkel cell polyomavirus

Eukaryotic cells synthesize proteins primarily through cap-dependent mRNA translation. This process is mediated by a complex of eukaryotic translation initiation factors, eIF4F, which assemble on the 7-methyl-guanosine cap of mRNA (1). eIF4E occupation of the 5′ cap of mRNA results in the recruitment of eIF4F complex members—mainly eIF4G, eIF4A, and eIF3—which in turn attract the 40S ribosome and the rest of the translation machinery (1). A set of small binding proteins called eIF4E-binding proteins (4E-BPs)—4E-BP1, 4E-BP2, and 4E-BP3—inhibit cap-dependent translation by interacting with the cap-bound eIF4E (2). The best-characterized and predominant eIF4E binding protein is 4E-BP1, which has a molecular weight of 15 kDa and is expressed in most tissues (2). 4E-BP1 competes with the complex scaffold protein eIF4G for the same binding site on eIF4E and prevents eIF4F cap complex assembly and ribosome recruitment (2, 3).

The PI3K-Akt (protein kinase B) pathway regulates the translation repressor function of 4E-BP1 by activating the mammalian target of rapamycin (mTOR) kinase (2, 3). Stimulated by metabolic and growth-related signals, mTOR phosphorylates 4E-BP1 and decreases its affinity for eIF4E in favor of translation (3). Priming phosphorylations at Thr(T)37 and T46 are required for subsequent phosphorylations at T70 and Ser(S)65 (3). Double alanine substitutions of the critical T37 and T46 priming sites render a constitutively active protein that strongly binds eIF4E and is insensitive to mTOR inhibition (4). Three additional potential phosphorylation sites have been identified—S83, S101, and S112—whose regulation mechanisms remain unclear (5–7).

Accumulating evidence indicates that dysregulation of cap-dependent translation through 4E-BP1 inactivation contributes to malignant transformation (2, 3). Frequently activated in cancers, the PI3K-Akt-mTOR pathway leads to enhanced 4E-BP1 phosphorylation and thus diminished translation repression activity (8–10); multiple reports have found expression of high levels of phosphorylated 4E-BP1 in tumors (3). Overexpression of eIF4E transforms cells by enhancing translation of oncogenic mRNA, which can be reversed by ectopic expression of a nonphosphorylatable 4E-BP1 priming site mutant (11–13). Resistance of various cancers to mTOR inhibitor treatment indicates that other pathways are implicated in 4E-BP1 inactivation (14). Several serine/threonine kinases have been shown to phosphorylate 4E-BP1, such as p38 MAPK, ERK, PIM2, ATM, CDK1, PLK1, LRRK2, GSK3β, and CK1ε (15–23). We recently demonstrated that cyclin-dependent kinase 1 (CDK1) phosphorylates 4E-BP1 at canonical sites T37, T46, S65, and T70 during mitosis and generates a high-molecular-weight phospho-isoform called δ-4E-BP1, even in the absence of mTOR activity (24). Although we have observed active cap-dependent translation during mitosis, the function of hyperphosphorylated δ-4E-BP1 and its contribution to tumorigenesis remain unknown.

Here we identify a CDK1 phosphorylation site, S83, that is unique to mitotic δ-4E-BP1. 4E-BP1 S83 phosphorylation does not participate in regulation of general cap-dependent translation or eIF4F complex formation. Instead, S83-phosphorylated δ-4E-BP1 preferentially localizes to mitotic centrosomes and peaks during metaphase. When S83 is substituted with alanine, 4E-BP1.S83A, to prevent δ-4E-BP1 formation, the

Significance

Eukaryotic translation initiation factor 4E-binding protein 1 (4E-BP1) hyperphosphorylation is implicated in various cancers. Mammalian target of rapamycin (mTOR) targeting of canonical sites—Thr37, Thr46, Ser65, and Thr70—inhibits 4E-BP1 translation repression activity and promotes protein synthesis, which in turn leads to overexpression of several cellular oncoproteins. In addition to the canonical sites, cyclin-dependent kinase 1 (CDK1) phosphorylates 4E-BP1 at Ser83 during mitosis, which interestingly does not affect translation. Rather, this phosphorylation site is permissive for Merkel cell polyomavirus small T viral oncoprotein-induced cell transformation. These findings shed light on a previously unidentified role for mitotic 4E-BP1 in cancer cell growth.

Author contributions: C.V., E.C., M.S., P.S.M., and Y.C. designed research; C.V., E.C., M.S., P.J.L.-O., L.P.v.S., M.A.G., and J.M.J. performed research; Y.C. contributed new reagents/analytic tools; C.V., E.C., M.S., J.M.J., P.S.M., and Y.C. analyzed data; and C.V., E.C., M.S., P.S.M., and Y.C. wrote the paper.

Reviewers: J.A.D., Dana-Farber Cancer Institute; N.S., McGill University.

The authors declare no conflict of interest.

Freely available online through the PNAS open access option.

[1]To whom correspondence may be addressed. Email: yc70@pitt.edu or psm9@pitt.edu.

This article contains supporting information online at www.pnas.org/lookup/suppl/doi:10.1073/pnas.1607768113/-/DCSupplemental.

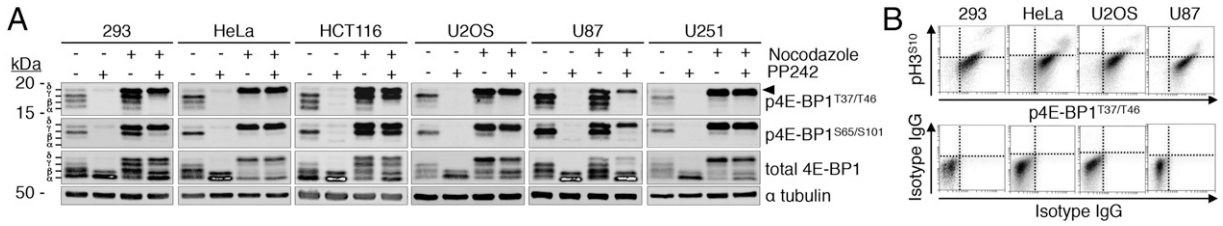

Fig. 1. δ-4E-BP1 hyperphosphorylation is a common feature of mitosis across multiple cancer cell lines. (*A*) Mitotic arrest of various cancer cell lines induces δ-4E-BP1. HEK293 (293), HeLa, HCT116, U2OS, U87, and U251 cells were arrested for 20 h with DMSO or nocodazole (prometaphase). Cells were treated at 16 h with mTOR kinase active site inhibitor PP242 (5 μM) for 4 h. Nocodazole arrest induces PP242-resistant δ-4E-BP1 (black arrowhead) in all cell lines tested. (*B*) $pH3^{S10+}$ mitotic cells have higher levels of $4E\text{-}BP1^{T37/T46}$ phosphorylation than interphase cells. Dual flow cytometry staining for $pH3^{S10}$ and $p4E\text{-}BP1^{T37/T46}$ was performed on asynchronous HEK293 (293), HeLa, U2OS, and U87 cells. Increased $pH3^{S10+}$ fluorescence was correlated to increased $p4E\text{-}BP1^{T37/T46+}$ fluorescence for all cell lines.

mutant 4E-BP1 partially inhibits cell transformation induced by the viral oncoprotein Merkel cell polyomavirus (MCV) small T (sT) antigen.

Results

δ-4E-BP1 Hyperphosphorylation Is a Feature of Mitosis Across Multiple Cancer Cell Lines. 4E-BP1 has four discernible gel isoforms named α, β, γ, and δ based on ascending molecular weight and phosphorylation (25). To determine the generalizability of δ-4E-BP1 expression during mitosis, six cell lines—HEK293, HeLa, HCT116, U2OS, U87, and U251—were arrested in prometaphase with nocodazole and examined for 4E-BP1 phosphorylation. Hyperphosphorylated δ-4E-BP1 was the predominant isoform in mitotic cells from all cell lines and is resistant to the mTOR inhibitor PP242 (Fig. 1*A*). Asynchronous cells expressed mainly α, β, and γ 4E-BP1 isoforms that were sensitive to mTOR inhibition. Expression of α, β, and γ forms was variably detectable and sensitive to PP242 in nocodazole-arrested cells, which is consistent with nonmitotic cell contamination. In addition, flow cytometry revealed a correlation between phospho-$4E\text{-}BP1^{T37/T46}$ ($p4E\text{-}BP1^{T37/T46}$) and mitotic marker phospho-histone $H3^{S10}$ ($pH3^{S10}$), indicating that mitotic cells tend to have a high level of 4E-BP1 phosphorylation (Fig. 1*B*).

S83 Phosphorylation Is a Component of δ-4E-BP1 and Is Mediated by CDK1. The phosphorylation of 4E-BP1 is hierarchical, with mTOR-directed priming phosphorylations at T37 and T46 being essential for additional phosphorylations at T70 and S65 (26). S65 phosphorylation is abundant in the γ-isoform in asynchronous cells, as well as the higher-molecular-weight δ-isoform during mitosis (Fig. 1*A*). λ Phosphatase treatment collapses all 4E-BP1 isoforms to the unphosphorylated form (24). These data are consistent with the δ-isoform having a unique phosphorylation site in addition to phosphorylations at other known sites. To identify additional phosphorylation sites responsible for the slower migration of the δ-isoform, HeLa and HEK293 cells arrested in mitosis, compared with asynchronous populations, were examined by LC-MS/MS–based quantitative phosphoproteome analysis. The phospho-S83 site represented by the digested peptide, ^{74}DLPTIPGVT(pS)PSSDEPPMEASQSHLR^{99}, was quantitatively identified only in mitotic cells (Fig. S1).

To confirm that phosphorylation at S83 is a bona fide component of the δ-4E-BP1 isoform, a phospho-specific antibody was raised in rabbits by immunizing with a synthetic 4E-BP1 peptide having S83 phosphorylated [^{77}TIPGVT(pS)PSSDEP^{89}]. This antiserum is specific for phospho-S83 but also has weak reactivity to nonphosphorylated 4E-BP1 that requires preabsorption or peptide blocking to reduce. Rabbit antiserum was screened by immunoblotting against lysates from asynchronous and mitotic HEK293 cells expressing HA-tagged 4E-BP1 variants—WT, T37A/T46A, S65A/S101A, T70A, and S83A (Tables S1 and S2). Immunoblotting showed loss of reactivity against only 4E-BP1.S83A expressed in mitotic cells, confirming the specificity of the antibody (Fig. S2). Phosphorylation of endogenous 4E-BP1 at T37, T46, S65, and T70 was present in α, β, and γ isoforms in asynchronous HeLa cells but not at S83 (Fig. 2*A*). S83 phosphorylation, however, was abundant only in the δ-4E-BP1 isoform of HeLa cells arrested with nocodazole. Reactivity of the δ-isoform with the other 4E-BP1 phospho-specific antibodies in the presence and absence of PP242 indicated that S83 phosphorylation occurs in addition to phosphorylation at other sites in δ-4E-BP1 and is resistant to mTOR inhibition. Asynchronous and mitotic HeLa cell lysates from Fig. 2*A* were also fractionated by 2D electrophoresis (Fig. 2*B*). S83 phosphorylation of 4E-BP1 was detected on the slowest-migrating isoelectric focusing spot corresponding to δ-4E-BP1 (white arrowheads) and a second spot (black arrowheads) below it that is absent in $p4E\text{-}BP1^{T37/T46}$ staining. In addition, a 4E-BP1.T37A/T46A priming-site mutant protein was phosphorylated at S83 but not at S65 in mitotic cells, indicating that phosphorylation at S83, in contrast to S65, may not be dependent on T37/T46 phosphorylation (Fig. 2*C*). Furthermore, S83 phosphorylation of 4E-BP1 in mitotic cells was confirmed by flow cytometry staining with $pH3^{S10}$ and $p4E\text{-}BP1^{S83}$ antiserum. U2OS (Fig. 2*D*) and HeLa (Fig. S3) cells showed $p4E\text{-}BP1^{S83}$ positivity exclusively for $pH3^{S10+}$ mitotic cells. When U2OS cells were arrested with nocodazole (Fig. 2*D*), mitotic cells formed a discrete $p4E\text{-}BP1^{S83+}/pH3^{S10+}$ population, indicating that nearly all mitotic cells express the δ-4E-BP1 isoform.

We have previously shown that proline-directed, serine/threonine kinase CDK1 phosphorylates 4E-BP1 during mitosis at T37/T46, S65/S101, and T70, all of which share the minimal consensus S/T-P sequence (24, 27). To determine whether CDK1 also phosphorylates S83, HeLa cells were arrested in G1 by L-mimosine treatment or in mitosis by nocodazole treatment and then treated with CDK1 active site inhibitor RO-3306, supplemented with MG132 proteasome inhibitor to prevent mitotic slippage (28, 29). CDK1 inhibition by RO-3306 abolished S83 phosphorylation and δ-4E-BP1 formation, in addition to reducing phosphorylation at the other phosphorylation sites (Fig. 2*E*). G1-arrested cells had low levels of phosphorylated 4E-BP1 that was sensitive to mTOR inhibition by PP242 but insensitive to RO-3306 (30). To confirm whether CDK1 directly phosphorylates S83, recombinant GST-4E-BP1 was mixed with mitotic HeLa lysate in an in vitro phosphorylation assay. The mitotic lysate phosphorylated GST-4E-BP1 at S83, which was reversed by addition of RO-3306 but not PP242, VX-680 (pan-AURK inhibitor), or BI-6727 (PLK1 kinase inhibitor) (Fig. 2*F*). Taken together, these findings demonstrate that CDK1 phosphorylates 4E-BP1 at S83 during mitosis.

S83-Phosphorylated 4E-BP1 Colocalizes with Centrosomes During Mitosis and Peaks at Metaphase. S83 phosphorylation of 4E-BP1 in mitotic cells was also confirmed by immunofluorescence microscopy. Staining of HEK293 (Fig. 3*A*), U2OS, HeLa, and U87 (Fig. S4) cells showed $p4E\text{-}BP1^{S83}$ positivity in all mitotic cells, which were also positive for $pH3^{S10}$, with the exception of telophase cells whose chromosomes are decondensed and hence negative for $pH3^{S10}$ (31). In addition to a diffuse staining pattern in mitotic cells, $p4E\text{-}BP1^{S83}$ also formed two distinct puncta near condensed chromosomes, which colocalized with centrosomal marker γ-tubulin as detected by confocal microscopy (Fig. 3*B*). To show that this binding is phospho-specific, we performed a

CELL BIOLOGY

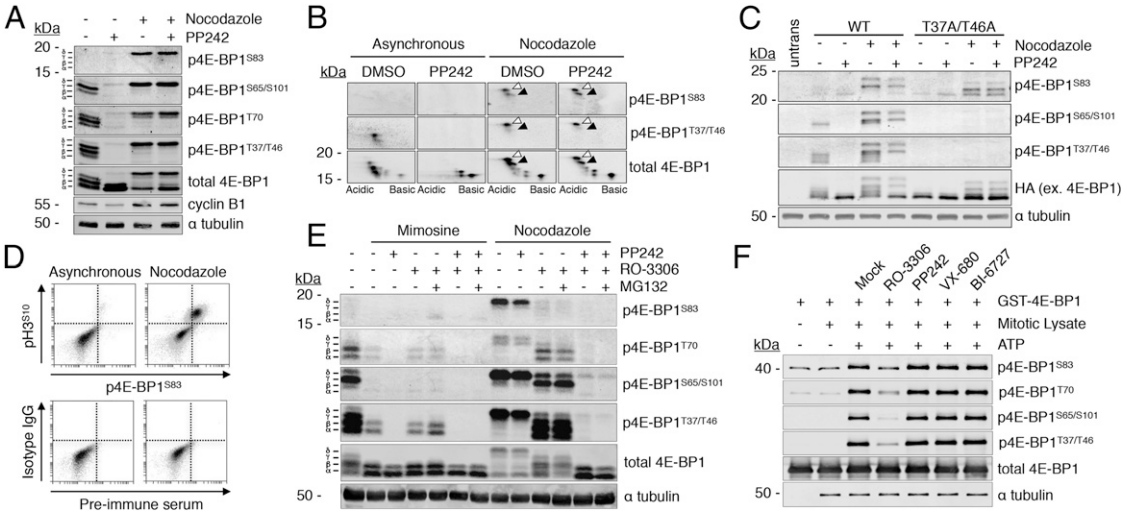

Fig. 2. S83 phosphorylation is a component of δ-4E-BP1 and is mediated by CDK1. (*A*) Polyclonal anti–p4E-BP1^{S83} rabbit antiserum detects S83 phosphorylation in mitotic δ-4E-BP1. HeLa lysates from asynchronous and nocodazole arrest conditions were immunoblotted with p4E-BP1^{S83} antiserum. p4E-BP1^{S83} was found only in the δ-4E-BP1 isoform in mitotic cells and was resistant to mTOR inhibition by PP242. (*B*) HeLa cell lysates from *A* were fractionated by isoelectric focusing (pH 3–6), followed by immunoblotting with phospho-specific and total 4E-BP1 antibodies. White arrowheads indicate the isoelectric focusing spot corresponding to δ-4E-BP1, and black arrowheads indicate a second spot revealed by p4E-BP1^{S83} staining. (*C*) Priming-site mutation of T37/T46 to alanine does not inhibit S83 phosphorylation during mitosis. WT and T37A/T46A mutant HA-4E-BP1 expression plasmids were transfected into HEK293 cells. Cells were arrested for 20 h with DMSO or nocodazole 48 h after transfection. Cells were treated at 16 h with mTOR kinase active site inhibitor PP242 (5 μM) for 4 h. Mutation of 4E-BP1 at T37/T46 blocked S65 phosphorylation but did not prevent S83 phosphorylation during mitosis. (*D*) pH3^{S10+} mitotic cells are positive for 4E-BP1^{S83} phosphorylation. Dual flow cytometry staining for pH3^{S10} and p4E-BP1^{S83} was performed on asynchronous and nocodazole-arrested U2OS cells. pH3^{S10} fluorescence was correlated to p4E-BP1^{S83}. (*E*) CDK1 inhibition by RO-3306 ablates S83 phosphorylation in mitotic cells. HeLa cells were arrested in G1 by L-mimosine treatment and mitosis by nocodazole treatment for 20 h. Cells were subsequently treated with kinase inhibitors PP242 (mTOR, 5 μM) and RO-3306 (CDK1, 9 μM) for 4 h, supplemented with 10 μM MG132 proteasome inhibitor to prevent mitotic exit/slippage. 4E-BP1^{S83} phosphorylation was abolished by RO-3306 treatment, along with δ-4E-BP1, in mitotic cells. Combined PP242 and RO-3306 erased most mitotic 4E-BP1 phosphorylation in these cells. S83 phosphorylation and δ-4E-BP1 were absent in G1-arrested cells, as expected. (*F*) Mitotic lysate phosphorylates GST-4E-BP1 at S83. Mitotic HeLa cell lysates enriched by nocodazole arrest were incubated with GST-4E-BP1 and reacted in buffer containing 200 μM ATP for 30 min at 30 °C in the presence or absence of mTOR (PP242), RO-3306 (CDK1), VX-680 (AURK A/B/C), and BI-6727 (PLK1) kinase inhibitors (5 μM). GST-4E-BP1 was phosphorylated at S83 and the other known regulatory sites. CDK1 inhibition by RO-3306 treatment reduces S83 phosphorylation, consistent with the other phosphorylation sites. Treatment with kinase inhibitors against other mitotic kinases AURK A/B/C and PLK1 did not inhibit S83 phosphorylation.

phospho-peptide competition assay for the staining (Fig. S5*A*). These data suggest that a portion of p4E-BP1^{S83} colocalize with centrosomes during mitosis. To further dissect the kinetics of mitotic 4E-BP1^{S83} phosphorylation, asynchronous HEK293 cells were counted in each of the phases of mitosis (pH3^{S10+}) and in interphase (pH3^{S10-}) based on their morphology and chromosome condensation. pH3^{S10} is present throughout mitosis but declines in telophase (31), while p4E-BP1^{S83} is low in prophase, peaks at metaphase, and also declines in telophase (Fig. 3*C*). Cells were also stained for p4E-BP1$^{T37/T46}$ but did not exhibit substantial differences across most phases (Fig. S6).

Mutation of 4E-BP1 at S83 Does Not Affect Total Cap-Binding and Cap-Dependent Translation but Partially Reverses MCV sT-Induced Rat-1 Cell Transformation. 4E-BP1 possesses an amino motif necessary for interaction with eIF4E, containing the sequence ^{54}YDRKFLM^{60} (32). The consensus binding motif Y(X)$_4$LΦ (where X is any amino acid residue and Φ is a hydrophobic residue) is shared by other 4E-BPs and translation initiation factor eIF4G. Recently, a C-terminal loop region of 4E-BP1, ^{78}PGVTS^{83}, was reported to also play an auxiliary role in binding eIF4E at a hydrophobic pocket separate from the canonical ^{54}YDRKFLM^{60} binding pocket (33–36). If S83 phosphorylation destabilizes this auxiliary domain, it may affect 4E-BP1:eIF4E interaction and cap-dependent initiation and translation.

To assess this, in vitro translation reactions were performed using the TNT transcription/translation coupled system with a bicistronic reporter having a firefly luciferase gene driven by cap-dependent translation followed by a renilla luciferase gene driven by cricket paralysis virus (CrPV) internal ribosome entry site (IRES)-mediated translation. Recombinant GST-tagged 4E-BP1.S83A decreased cap-dependent translation to similar levels as WT GST-tagged 4E-BP1, and CDK1 phosphorylation of this protein rescued translation (Fig. S7*A*). GST-4E-BP1.T37A/T46A having substitutions at priming sites inhibited translation despite CDK1 treatment. IRES-mediated translation, however, was unaffected by GST-4E-BP1 as expected (Fig. S7*B*). Similarly, 4E-BP1.S83A had no detectable effect on 7-methylguanosine 5′-triphosphate (m^{7}GTP) cap resin pull-down assays compared with WT 4E-BP1 protein (37). Compared with WT 4E-BP1, S83A (or phosphomimetic mutants S83D and S83E), did not differ significantly in binding cap-bound eIF4E and did not significantly affect cap-complex formation, as measured by eIF4G and eIF4A pull-down (Fig. 4*A*). Unlike 4E-BP1.S83A, phosphorylation-defective and raptor-binding mutants (T37A/T46A and I15A/F114A) efficiently inhibited eIF4G binding to eIF4E and in vitro cap-dependent translation (32, 38–40), suggesting that S83 phosphorylation does not play a significant role in general cap-dependent translation regulation.

MCV sT transforms Rat-1 and NIH 3T3 cells through a previously unidentified mechanism initiating mitotic 4E-BP1 phosphorylation that can be reversed by expression of a constitutively active 4E-BP1.T37A/T46A mutant (24, 41). To determine whether S83 phosphorylation is required for the transformation activity of this viral oncoprotein, we performed foci formation assays with Rat-1 coexpressing MCV sT and 4E-BP1 variants (Table S2). Cells were first stably transduced with empty vector, WT 4E-BP1, 4E-BP1.T37A/T46A, 4E-BP1.I15A/F114A, or 4E-BP1.S83A, followed by transduction with empty vector or MCV sT. MCV sT transformed Rat-1 cells expressing either empty vector control or WT 4E-BP1, and this was reversed by coexpression of nonphosphorylatable 4E-BP1.T37A/T46A and 4E-BP1.I15A/F114A mutant proteins (Fig. 4*B*). 4E-BP1.S83A mutant expression partially but reproducibly

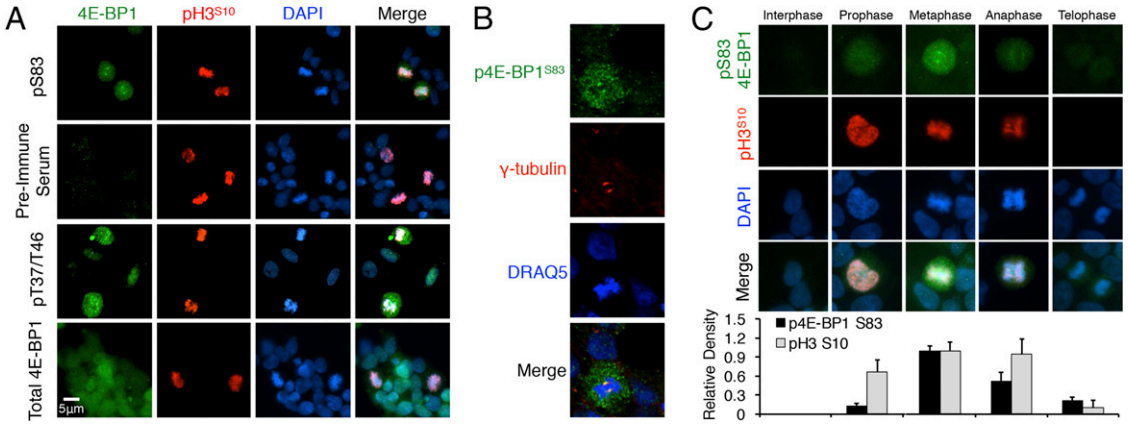

Fig. 3. S83-phosphorylated 4E-BP1 colocalizes with centrosomes during mitosis and peaks at metaphase. (*A*) Immunofluorescence staining shows the presence of p4E-BP1^{S83} only in mitotic cells. Asynchronous HEK293 cells were fixed and dual-stained with p4E-BP1^{S83} antiserum (green) and pH3^{S10} (red) antibodies. Nuclear DAPI stain is shown in blue. (*B*) p4E-BP1^{S83} staining colocalizes with γ-tubulin staining to centrosomes in mitotic nuclei of HEK293 cells. Asynchronous HEK293 cells were fixed and dual-stained with p4E-BP1^{S83} antiserum (green) and γ-tubulin (red) antibodies. Nuclear DRAQ5 stain is shown in blue. Stained cells were observed by confocal microscopy for colocalization studies. (*C*) 4E-BP1 S83 phosphorylation peaks at metaphase and declines in telophase. Asynchronous HEK293 cells were fixed and dual-stained with p4E-BP1^{S83} antiserum (green) and pH3^{S10} (red) antibodies. Nuclear DAPI stain is shown in blue. Cells in interphase and in different phases of mitosis (prophase, metaphase, anaphase, and telophase) were identified by morphology and chromosome condensation. Intensity of p4E-BP1^{S83} staining for cells in each phase was quantified by ImageJ. Thirty cells for each phase were quantified, and averages for three independent experiments with SEM are shown.

decreased sT-induced transformation to ∼51% of empty vector control and ∼66% of WT 4E-BP1. Immunoblotting of lysates from these cells show comparable protein levels of WT 4E-BP1 and 4E-BP1.S83A; therefore, the negative effect on foci formation did not result from enhanced expression of the latter (Fig. S8). Low protein levels were predictably observed for 4E-BP1.T37A/T46A and 4E-BP1.I15A/F114A mutants because they inhibit their own translation.

Discussion

During mitosis, 4E-BP1 is hyperphosphorylated, rendering it inactive as a cap-dependent translation gate keeper (24). Our current studies show that S83-phosphorylated δ-4E-BP1 is specific to mitosis and is a result of CDK1 activity. When S83 is mutated to a nonphosphorylatable alanine, no changes in cap-binding or cap-dependent translation were detected. Instead, loss of this phosphorylation site partially reverses cell transformation caused by the MCV small T oncoprotein. Unlike α-γ phosphorylated 4E-BP1 isoforms, δ-4E-BP1 accumulates at centrosomes during mitosis. Unlike 4E-BP1 phosphorylation by mTOR kinase at canonical sites, CDK1 phosphorylation of 4E-BP1 at S83 may lead to a gain-of-function for this hyperphosphorylated protein. We only find evidence for S83 phosphorylation and accumulation of the δ-4E-BP1 isoform during mitosis. Previous studies suggesting that S83 phosphorylation can occur in adipocytes treated with insulin (5) are best explained by increased mitogenesis rather than direct kinase signaling. We find in recombinant protein enzyme assays that CDK1/CYCB directly phosphorylates 4E-BP1, but it is possible that other CDK1 partners (e.g., CYCA) may also direct 4E-BP1 hyperphosphorylation.

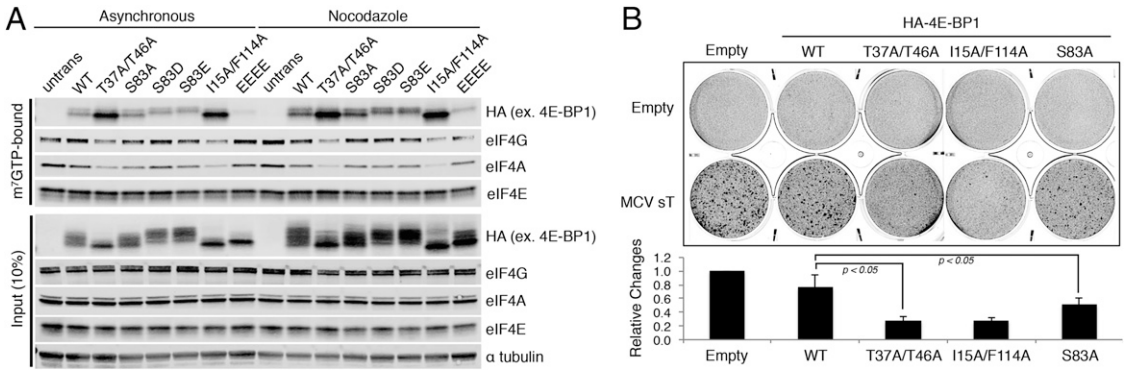

Fig. 4. Mutation of 4E-BP1 at S83 does not affect general cap-dependent translation initiation complex formation but partially reverses MCV sT-induced Rat-1 cell transformation. (*A*) eIF4F cap-binding is not affected by S83 phosphorylation. HEK293 cells were transfected with WT HA-tagged 4E-BP1 and mutants T37A/T46A, S83A, S83D, S83E, I15A/F114A, and T37E/T46E/S65E/T70E (EEEE) (Tables S1 and S2). After 48 h, cells were treated with DMSO or nocodazole for 20 h and harvested. Cell lysates were either directly immunoblotted (input) or mixed with m^{7}GTP coupled Sepharose beads, precipitated, and immunoblotted. S83A, S83D, and S83D mutants did not differ from WT 4E-BP1 in their binding to cap-bound eIF4E and did not affect eIF4G and eIF4A association to eIF4E. HA-4E-BP1 phosphorylation mutant T37A/T46A and raptor-binding mutant I15A/F114A reduced eIF4G and eIF4A binding, whereas the opposite pattern was found for negative control phosphomimetic mutant EEEE. Comparable amounts of eIF4G and eIF4A were pulled down with m^{7}GTP beads for both asynchronous and mitotic cells. (*B*) A representative foci formation assay with the MCV sT viral oncoprotein in Rat-1 cells stably expressing HA-tagged 4E-BP1 WT, T37A/T46A, I15A/F114A, and S83A mutants, and empty vector (Table S2). Foci formed 2 wk after MCV sT lentivirus transduction were stained with 0.5% crystal violet. Crystal violet staining intensity was measured using the LICOR infrared scanner. For each stable cell line, crystal violet staining intensity of empty vector-transduced cells was subtracted from that of sT-transduced cells, and relative intensity to empty vector control was determined for each HA-4E-BP1 mutant. Results are mean ± SD from three independent experiments. One-sided *t* test was performed to determine significance.

Our findings confirm previous studies showing δ-4E-BP1 expression in multiple cell lines synchronized in mitosis by chemical or mechanical means (16, 42). Treatment with nocodazole, a microtubule-destabilizing drug, induced δ-4E-BP1 across all cell lines. Although mTOR inhibition by PP242 eliminates most phosphorylated 4E-BP1 isoforms in asynchronous cells, it does not affect δ-4E-BP1. The appearance of α, β, and γ forms of 4E-BP1 in nocodazole-arrested cells is likely due to interphase cell contamination resulting from differences in synchronization efficiency between cell lines, which would explain their sensitivity to PP242 treatment. As predicted by immunoblotting, flow cytometry analysis of all cell lines tested shows that $pH3^{S10+}$ mitotic cells exhibit higher levels of $p4E\text{-}BP1^{T37/T46+}$ than $pH3^{S10-}$ interphase cells.

Because of its low abundance in asynchronous cells, S83 phosphorylation has not been thus far amenable to investigation in contrast to the canonical mTOR-regulated sites—T37, T46, S65, and T70 (5). We hypothesized that δ-4E-BP1 from mitotic cells has additional phosphorylation sites that have been missed in previous analyses where mitotic cells comprise less than 1% of all cells in bulk culture. We subjected interphase (mitosis-depleted) and mitotic (mitosis-enriched) HeLa and HEK293 cells for MS analysis and identified S83 phosphorylation exclusively in mitotic cells. Mutation of mTOR priming sites T37A/T46A did not inhibit S83 phosphorylation in mitotic cells, suggesting that S83 targeting may not rely on mTOR activity as also evidenced by PP242-mediated mTOR inhibition. Our epitope-tagged 4E-BP1 construct does not migrate the same way as endogenous 4E-BP1 and makes it difficult to assess each phospho-isoform discretely. Nonetheless, we are confident that the highest molecular weight form of HA-tagged 4E-BP1 induced during mitosis represents δ-4E-BP1.

By generating a polyclonal antibody against $p4E\text{-}BP1^{S83}$, we were able to confirm that δ-4E-BP1 is phosphorylated at S83 and that this antibody can be used as a mitotic marker for immunoblotting, immunofluorescence, and flow cytometry. We were also able to localize a portion of S83-phosphorylated 4E-BP1 at the centrosomes consistent with a previous report, which shows that 4E-BP1 knockdown leads to multipolar spindles and misaligned chromosomes (23). Further, S83 phosphorylation increased from prophase to metaphase and decreased thereafter, which is in agreement with nocodazole prometaphase synchronization results and with the timing of CDK1 activity (27).

The $p4E\text{-}BP1^{S83}$ antibody also enabled us to determine that CDK1 is the first kinase known to phosphorylate 4E-BP1 at the five phospho-residues (T37, T46, S65, T70, and S83) conserved in both 4E-BP1 and 4E-BP2 (2). The polyclonal $p4E\text{-}BP1^{S83}$ antiserum has cross-reactivity against nonphosphorylated S83 that requires preabsorption or peptide blocking, which would explain why unreacted GST-4E-BP1 can still be detected in our in vitro phosphorylation assays. However, the substantial increase in $p4E\text{-}BP1^{S83}$ signal in ATP-supplemented reactions confirms our in vivo results. Epitope competition assay with dephosphorylated GST-4E-BP1 also shows that the antiserum is specific for S83-phosphorylated 4E-BP1 (Fig. S5*B*). Nevertheless, all immunofluorescence colocalization studies were performed using antiserum preabsorbed with nonphosphorylated peptide ^{77}TIPGVTSPSSDEP^{89}.

Others have reported and established modulation of cap-dependent translation through 4E-BP1 phosphorylation at mTOR-targeted sites. Using in vitro translation and m^7GTP cap-affinity pulldown assays, we do not find general cap-dependent translation regulation by 4E-BP1 S83 phosphorylation. Although we did not find S83 phosphorylation affecting general cap-binding or cap-dependent translation, we cannot exclude the possibility that an mRNA subpopulation is regulated by S83-phosphorylated 4E-BP1, such as terminal oligopyrimidine tract (TOP)-containing mRNAs that are reported to be translationally active during mitosis (43). A recent study shows that the interaction between the C-terminal loop with eIF4E is required for eIF4F complex formation and translation repression in vivo using 4E-BP1 truncation mutants, which, in light of our results, prompts the examination of other loop residues (36). Expression of full-length 4E-BP1 constructs with mutations at canonical and noncanonical eIF4E binding motifs would provide robust evidence for this phenomenon in cells.

Overexpression of constitutively active 4E-BP1 or 4E-BP2 antagonizes cell transformation induced by eIF4E, v-Src, H-Ras, and MCV sT, indicating that 4E-BP1 acts as a tumor suppressor (41, 44, 45). Expression of S65A and T70A have also been reported to decrease cloned rat embryo fibroblast (CREF) colony formation, but these results were not confirmed in the presence of an oncogene (46). Our work showing partial reversal of sT-mediated foci formation indicates that the 4E-BP1 phosphorylation site S83 contributes to that MCV sT cell transformation activity. sT transformation is eliminated by a raptor-binding mutant of 4E-BP1 (38-40), suggesting that mTOR and CDK1 cooperatively promote sT-induced cell transformation. These findings hint at the possibility that this residue is also permissive for cell transformation induced by other oncoproteins that promote mitogenesis.

Hyperphosphorylation of 4E-BP1 in various cancers has been strongly suggestive of uncontrolled protein synthesis. However, our study provokes a reassessment of the role of 4E-BP1 in cells, particularly during mitosis. It is possible that the S83-phosphorylated δ-4E-BP1 isoform has a previously undescribed gain-of-function role in mitosis.

Materials and Methods

No human subjects were used in experiments and the rabbit anti–phospho-Ser83 polyclonal antibody was generated against the 4E-BP1 synthetic peptide (see below) by Rockland Immunochemicals Inc. Plasmids, antibodies, primers, and standard methods are described in *SI Materials and Methods*.

Cell Cycle Synchronization. HeLa, HCT116, U2OS, HEK293 (ATCC), U87, and U251 cells (obtained from H. Okada, University of California San Francisco, San Francisco, CA) were synchronized as previously described (24).

Kinase Inhibitors. Active site kinase inhibitors were used in cell culture as follows: 5 μM PP242 (mTOR) and 9 μM RO-3306 (CDK1). Proteasome inhibitor MG132 (10 μM) was coincubated with RO-3306 for in vivo CDK1 inhibition. PP242, RO-3306, VX-680 (AURK), and BI-6727 (PLK1) kinase inhibitors were used at 5 μM for in vitro phosphorylation assays.

Phospho-Ser83 4E-BP1 Polyclonal Antibody Production. Rabbits were immunized with 4E-BP1 synthetic phospho-peptide ^{77}TIPGVT(pS)PSSDEP^{89}. Antiserum was periodically collected after multiple immunization boosts.

Flow Cytometry. Asynchronous U2OS, U87, HeLa, and HEK293 cells were trypsinized, fixed in 10% buffered formalin, and permeabilized with 0.1% saponin in 1% FBS/PBS for 15 min at room temperature. Cells were stained with $p4E\text{-}BP1^{T37/T46}$ antibody or rabbit IgG control antibody for 3 h at room temperature. After washing three times with 1% FBS/PBS, cells were reacted with anti-rabbit Alexa 488-labeled IgG (Invitrogen) for 1 h at room temperature. For phospho-histone $H3^{S10}$ staining, cells were permeabilized with 1% FBS/PBS containing 0.25% Triton X-100 for 3 min at room temperature. Alexa 647-labeled $pH3^{S10}$ antibody (Cell Signaling) or control Alexa 647-labeled rabbit IgG (Cell Signaling) was reacted with cells for 1 h at room temperature. After washing three times with 1% FBS/PBS, DNA was stained with 1% FBS/PBS containing 50 μg/mL propidium iodide (PI) and 40 μg/mL RNase A (Sigma) for 30 min. For $p4E\text{-}BP1^{S83}$ flow cytometry analysis, U2OS and HeLa cells were treated with growth medium containing 0.5 μM nocodazole or DMSO for 20 h. $p4E\text{-}BP1^{S83}$ antiserum or preimmune serum in 1% FBS/PBS was used. Cells were analyzed by the BD Accuri C6 cell analyzer (BD Biosciences).

MS. HeLa cells were disrupted, and proteins were tryptically digested, phosphopeptide enriched, TMT10 labeled, and high mass accuracy LC-MS/MS analyzed as previously described (47). Variations include use of TMT10 instead of iTRAQ labeling, cell lysate vs. tissue disruption, and use of Q Exactive Orbitrap MS. HEK293 cell LC-MS/MS analyses were performed identically, except for quantitation that used label-free approaches as previously described (48).

2D Electrophoresis. HeLa cells were lysed in nondenaturing lysis buffer supplemented with protease inhibitors (Roche). Lysates were isoelectrically focused as previously described (24).

In Vitro Protein Phosphorylation Assay. Recombinant GST-4E-BP1 was incubated in a reaction containing 1× protein kinase buffer (NEB) and mitotic HeLa cell lysate as previously described (24).

Immunofluorescence. HEK293, HeLa, U2OS, or U87 cells (0.3×10^6) were seeded onto poly-L-lysine–treated glass coverslips. The next day, cells were washed with ice-cold 1× PBS and fixed with 2% paraformaldehyde for 15 min at room temperature, followed by permeabilization with cold MetOH for 10 min at −20 °C. Cells were blocked with 10% normal goat serum (Cell Signaling) for 1 h at room temperature and then stained with p4E-BP1^{S83} antiserum preabsorbed with unphosphorylated ^{77}TIPGVTSPSSDEP^{89}, together with γ-tubulin or phospho-histone H3^{S10} antibodies (Cell Signaling) for 2 h at room temperature. Cells were then washed with cold 1× PBS three times for 5 min each and incubated with Alexa 488-labeled anti-rabbit secondary antibody and Alexa 568-labeled anti-mouse antibody (Invitrogen) at room temperature for 1 h. Cells were examined by fluorescence microscopy (Olympus). Confocal microscopy was performed with Leica TCS SP2 upright confocal microscope. Intensity of fluorescence staining was measured by ImageJ (NIH).

m^{7}GTP Cap Binding Assay. HEK293 cells were lysed in nondenaturing lysis buffer supplemented with protease inhibitors (Roche). Lysates were incubated with m^{7}GTP Sepharose beads (Jena Bioscience) as previously described (24).

Foci Formation Assays. To determine viral titer and establish stable cell lines, Rat-1 cells were infected with pLVX EF HA-4E-BP1 lentiviruses and selected with puromycin (2 μg/mL). Rat-1 cells stably expressing various HA-4E-BP1 proteins were infected with pLVX EF MCV sT lentivirus and grown for 2 wk in six-well plates. Foci were stained with crystal violet (0.025% in 1× PBS), and plates were photographed and scanned with an Odyssey scanner (LI-COR) for quantification.

ACKNOWLEDGMENTS. We thank Ornette Coleman and Ann Southam for help in preparing the manuscript. This work was supported by NIH National Cancer Institute Grants R01CA136806, CA136363, CA170354, and 1R35CA197463-01 and American Cancer Society professorships to Y.C. and P.S.M. This project used the University of Pittsburgh Cancer Institute Cytometry Facility and LI-COR Imaging Facility, supported in part by NIH Grant P30CA047904. This project is funded, in part, under a grant with the Pennsylvania Department of Health. Portions of this research were supported by the NIH National Institute of General Medical Sciences (GM103493) and the W.R. Wiley Environmental Molecular Science Laboratory. Pacific Northwest National Laboratory is operated by Battelle Memorial Institute for the US Department of Energy under Contract DE-AC05-76RLO-1830.

1. Jackson RJ, Hellen CU, Pestova TV (2010) The mechanism of eukaryotic translation initiation and principles of its regulation. *Nat Rev Mol Cell Biol* 11(2):113–127.
2. Martineau Y, Azar R, Bousquet C, Pyronnet S (2013) Anti-oncogenic potential of the eIF4E-binding proteins. *Oncogene* 32(6):671–677.
3. Musa J, et al. (February 1, 2016) Eukaryotic initiation factor 4E-binding protein 1 (4E-BP1): A master regulator of mRNA translation involved in tumorigenesis. *Oncogene*, 10.1038/onc.2015.515.
4. Gingras AC, et al. (1999) Regulation of 4E-BP1 phosphorylation: A novel two-step mechanism. *Genes Dev* 13(11):1422–1437.
5. Fadden P, Haystead TA, Lawrence JC, Jr (1997) Identification of phosphorylation sites in the translational regulator, PHAS-I, that are controlled by insulin and rapamycin in rat adipocytes. *J Biol Chem* 272(15):10240–10247.
6. Wang X, Li W, Parra JL, Beugnet A, Proud CG (2003) The C terminus of initiation factor 4E-binding protein 1 contains multiple regulatory features that influence its function and phosphorylation. *Mol Cell Biol* 23(5):1546–1557.
7. Heesom KJ, Avison MB, Diggle TA, Denton RM (1998) Insulin-stimulated kinase from rat fat cells that phosphorylates initiation factor 4E-binding protein 1 on the rapamycin-insensitive site (serine-111). *Biochem J* 336(Pt 1):39–48.
8. Mamane Y, Petroulakis E, LeBacquer O, Sonenberg N (2006) mTOR, translation initiation and cancer. *Oncogene* 25(48):6416–6422.
9. Sabatini DM (2006) mTOR and cancer: Insights into a complex relationship. *Nat Rev Cancer* 6(9):729–734.
10. Wang X, Proud CG (2011) mTORC1 signaling: What we still don't know. *J Mol Cell Biol* 3(4):206–220.
11. Lazaris-Karatzas A, Montine KS, Sonenberg N (1990) Malignant transformation by a eukaryotic initiation factor subunit that binds to mRNA 5′ cap. *Nature* 345(6275):544–547.
12. Avdulov S, et al. (2004) Activation of translation complex eIF4F is essential for the genesis and maintenance of the malignant phenotype in human mammary epithelial cells. *Cancer Cell* 5(6):553–563.
13. De Benedetti A, Graff JR (2004) eIF-4E expression and its role in malignancies and metastases. *Oncogene* 23(18):3189–3199.
14. Carew JS, Kelly KR, Nawrocki ST (2011) Mechanisms of mTOR inhibitor resistance in cancer therapy. *Target Oncol* 6(1):17–27.
15. Herbert TP, Tee AR, Proud CG (2002) The extracellular signal-regulated kinase pathway regulates the phosphorylation of 4E-BP1 at multiple sites. *J Biol Chem* 277(13):11591–11596.
16. Heesom KJ, Gampel A, Mellor H, Denton RM (2001) Cell cycle-dependent phosphorylation of the translational repressor eIF-4E binding protein-1 (4E-BP1). *Curr Biol* 11(17):1374–1379.
17. Shin S, Wolgamott L, Roux PP, Yoon SO (2014) Casein kinase 1ε promotes cell proliferation by regulating mRNA translation. *Cancer Res* 74(1):201–211.
18. Shin S, et al. (2014) Glycogen synthase kinase-3β positively regulates protein synthesis and cell proliferation through the regulation of translation initiation factor 4E-binding protein 1. *Oncogene* 33(13):1690–1699.
19. Liu G, Zhang Y, Bode AM, Ma WY, Dong Z (2002) Phosphorylation of 4E-BP1 is mediated by the p38/MSK1 pathway in response to UVB irradiation. *J Biol Chem* 277(11):8810–8816.
20. Yang DQ, Kastan MB (2000) Participation of ATM in insulin signalling through phosphorylation of eIF-4E-binding protein 1. *Nat Cell Biol* 2(12):893–898.
21. Imai Y, et al. (2008) Phosphorylation of 4E-BP by LRRK2 affects the maintenance of dopaminergic neurons in Drosophila. *EMBO J* 27(18):2432–2443.
22. Fox CJ, et al. (2003) The serine/threonine kinase Pim-2 is a transcriptionally regulated apoptotic inhibitor. *Genes Dev* 17(15):1841–1854.
23. Shang ZF, et al. (2012) 4E-BP1 participates in maintaining spindle integrity and genomic stability via interacting with PLK1. *Cell Cycle* 11(18):3463–3471.
24. Shuda M, et al. (2015) CDK1 substitutes for mTOR kinase to activate mitotic cap-dependent protein translation. *Proc Natl Acad Sci USA* 112(19):5875–5882.
25. Gingras AC, Kennedy SG, O'Leary MA, Sonenberg N, Hay N (1998) 4E-BP1, a repressor of mRNA translation, is phosphorylated and inactivated by the Akt(PKB) signaling pathway. *Genes Dev* 12(4):502–513.
26. Gingras AC, et al. (2001) Hierarchical phosphorylation of the translation inhibitor 4E-BP1. *Genes Dev* 15(21):2852–2864.
27. Enserink JM, Kolodner RD (2010) An overview of Cdk1-controlled targets and processes. *Cell Div* 5:11.
28. Vassilev LT, et al. (2006) Selective small-molecule inhibitor reveals critical mitotic functions of human CDK1. *Proc Natl Acad Sci USA* 103(28):10660–10665.
29. Skoufias DA, Indorato RL, Lacroix F, Panopoulos A, Margolis RL (2007) Mitosis persists in the absence of Cdk1 activity when proteolysis or protein phosphatase activity is suppressed. *J Cell Biol* 179(4):671–685.
30. Feldman ME, et al. (2009) Active-site inhibitors of mTOR target rapamycin-resistant outputs of mTORC1 and mTORC2. *PLoS Biol* 7(2):e38.
31. Li DW, et al. (2005) Dynamic distribution of Ser-10 phosphorylated histone H3 in cytoplasm of MCF-7 and CHO cells during mitosis. *Cell Res* 15(2):120–126.
32. Mader S, Lee H, Pause A, Sonenberg N (1995) The translation initiation factor eIF-4E binds to a common motif shared by the translation factor eIF-4 gamma and the translational repressors 4E-binding proteins. *Mol Cell Biol* 15(9):4990–4997.
33. Paku KS, et al. (2012) A conserved motif within the flexible C-terminus of the translational regulator 4E-BP is required for tight binding to the mRNA cap-binding protein eIF4E. *Biochem J* 441(1):237–245.
34. Gosselin P, et al. (2011) The translational repressor 4E-BP called to order by eIF4E: New structural insights by SAXS. *Nucleic Acids Res* 39(8):3496–3503.
35. Peter D, et al. (2015) Molecular architecture of 4E-BP translational inhibitors bound to eIF4E. *Mol Cell* 57(6):1074–1087.
36. Sekiyama N, et al. (2015) Molecular mechanism of the dual activity of 4EGI-1: Dissociating eIF4G from eIF4E but stabilizing the binding of unphosphorylated 4E-BP1. *Proc Natl Acad Sci USA* 112(30):E4036–E4045.
37. Webb NR, Chari RV, DePillis G, Kozarich JW, Rhoads RE (1984) Purification of the messenger RNA cap-binding protein using a new affinity medium. *Biochemistry* 23(2):177–181.
38. Schalm SS, Fingar DC, Sabatini DM, Blenis J (2003) TOS motif-mediated raptor binding regulates 4E-BP1 multisite phosphorylation and function. *Curr Biol* 13(10):797–806.
39. Beugnet A, Wang X, Proud CG (2003) Target of rapamycin (TOR)-signaling and RAIP motifs play distinct roles in the mammalian TOR-dependent phosphorylation of initiation factor 4E-binding protein 1. *J Biol Chem* 278(42):40717–40722.
40. Choi KM, McMahon LP, Lawrence JC, Jr (2003) Two motifs in the translational repressor PHAS-I required for efficient phosphorylation by mammalian target of rapamycin and for recognition by raptor. *J Biol Chem* 278(22):19667–19673.
41. Shuda M, Kwun HJ, Feng H, Chang Y, Moore PS (2011) Human Merkel cell polyomavirus small T antigen is an oncoprotein targeting the 4E-BP1 translation regulator. *J Clin Invest* 121(9):3623–3634.
42. Greenberg VL, Zimmer SG (2005) Paclitaxel induces the phosphorylation of the eukaryotic translation initiation factor 4E-binding protein 1 through a Cdk1-dependent mechanism. *Oncogene* 24(30):4851–4860.
43. Park JE, Yi H, Kim Y, Chang H, Kim VN (2016) Regulation of Poly(A) Tail and Translation during the Somatic Cell Cycle. *Mol Cell* 62(3):462–471.
44. Rousseau D, Gingras AC, Pause A, Sonenberg N (1996) The eIF4E-binding proteins 1 and 2 are negative regulators of cell growth. *Oncogene* 13(11):2415–2420.
45. She QB, et al. (2010) 4E-BP1 is a key effector of the oncogenic activation of the AKT and ERK signaling pathways that integrates their function in tumors. *Cancer Cell* 18(1):39–51.
46. Li S, et al. (2002) Translational control of cell fate: Availability of phosphorylation sites on translational repressor 4E-BP1 governs its proapoptotic potency. *Mol Cell Biol* 22(8):2853–2861.
47. Mertins P, et al. (2014) Ischemia in tumors induces early and sustained phosphorylation changes in stress kinase pathways but does not affect global protein levels. *Mol Cell Proteomics* 13(7):1690–1704.
48. Brown JN, et al. (2012) Morphine produces immunosuppressive effects in nonhuman primates at the proteomic and cellular levels. *Mol Cell Proteomics* 11(9):605–618.